Biomed Microdevices (2011) 13:159–167
DOI 10.1007/s10544-010-9481-7

Asymmetry of blood flow and cancer cell adhesion in a microchannel with symmetric bifurcation and confluence

Takuji Ishikawa · Hiroki Fujiwara · Noriaki Matsuki · Takefumi Yoshimoto · Yohsuke Imai · Hironori Ueno · Takami Yamaguchi

Published online: 20 October 2010

Abstract Bifurcations and confluences are very common geometries in biomedical microdevices. Blood flow at microchannel bifurcations has different characteristics from that at confluences because of the multiphase properties of blood. Using a confocal micro-PIV system, we investigated the behaviour of red blood cells (RBCs) and cancer cells in microchannels with geometrically symmetric bifurcations and confluences. The behaviour of RBCs and cancer cells was strongly asymmetric at bifurcations and confluences whilst the trajectories of tracer particles in pure water were almost symmetric. The cell-free layer disappeared on the inner wall of the bifurcation but increased in size on the inner wall of the confluence. Cancer cells frequently adhered to the inner wall of the bifurcation but rarely to other locations. Because the wall surface coating and the wall shear stress were almost symmetric for the bifurcation and the confluence, the result indicates that not only chemical mediation and wall shear stress but also microscale haemodynamics play important roles in the adhesion of cancer cells to the microchannel walls. These results provide the fundamental basis for a better understanding of blood flow and cell adhesion in biomedical microdevices.

Keywords Microchannel · Blood flow · Red blood cells · Cancer cells · Bifurcation · Confluence

Electronic supplementary material The online version of this article (doi:10.1007/s10544-010-9481-7) contains supplementary material, which is available to authorized users.

T. Ishikawa (✉) · H. Fujiwara · T. Yoshimoto · Y. Imai
Department of Bioengineering and Robotics,
Graduate School of Engineering, Tohoku University,
6-6-01, Aoba, Aramaki, Aoba-ku,
Sendai 980-8579, Japan
e-mail: ishikawa@pfsl.mech.tohoku.ac.jp

N. Matsuki · T. Yamaguchi
Department of Biomedical Engineering,
Graduate School of Biomedical Engineering, Tohoku University,
6-6-01 Aoba,
Sendai 980-8579, Japan

H. Ueno
International Advanced Research and Education Organization,
Tohoku University,
6-6-01 Aoba,
Sendai 980-8579, Japan

1 Introduction

Blood is a concentrated suspension of blood cells in plasma, and about 99% of the volume fraction of blood cells consists of red blood cells (RBCs). When blood flows in a microchannel with a diameter of less than about 50 μm, the size of the RBCs is comparable to that of the generated flow field. Under such conditions, blood can no longer be assumed to be homogeneous and must be treated as a multiphase fluid. In a straight capillary tube, the apparent viscosity of blood decreases with the tube diameter, a phenomenon known as the Fahraeus–Lindqvist effect (Fahraeus and Lindqvist 1931). This effect can be explained by the migration of RBCs towards the core flow and the increase of the relative thickness of the cell-free layer. Such microscale haemodynamics play an important role in the transport phenomena in various biomedical microdevices. In the case of microchannels with complex geometries, however, microscale haemodynamics are still not well understood.

We previously investigated the motion of RBCs in a straight tube (Lima et al. 2008) and in a microchannel with

stenosis (Fujiwara et al. 2009) using a confocal micro-PIV (particle image velocimetry) system. That research showed that the channel geometry strongly affected the mixing of RBCs. Although bifurcation and confluence are very common geometries in biomedical microdevices, the detailed haemodynamics in these geometries are still unclear. The flow field for Stokes flow of a homogeneous Newtonian fluid is symmetric between the bifurcation and the confluence if the geometry is symmetric. For blood, however, the flow field exhibits different characteristics in the bifurcation and the confluence, which are the subjects of this paper.

Microscale haemodynamics may also play an important role in the adhesion of cells on microchannel walls. In former medical researches, adhesion phenomena on blood vessel walls have been investigated in great detail for leukocytes (e.g., Ostermann et al. 2002; DiVietro et al. 2007), malaria-infected RBCs (e.g., Scholander et al. 1996; Beeson et al. 2000) and cancer cells (e.g., Miles et al. 2008; Glinskii et al. 2005; Mine et al. 2003; Fidler 2003; Chambers et al. 2002). The effect of shear stress on the adhesion of cancer cells has also been thoroughly investigated (Bastida et al. 1989; Moss et al. 1999; Kitayama et al. 2000; Thamilselvan et al. 2004; Liang et al. 2005, 2008). Although these results provide evidence of the complex role of haemodynamic forces in the recruitment of metastatic cancer cells to endothelial cell, they do not provide enough information on how the channel geometry affects the adhesion phenomena.

Recently, a wide variety of microfluidic devices have been developed for efficient cell separation. Micropillar arrays were used by Tan et al. (2009) and Mohamed et al. (2009) to isolate circulating tumour cells from blood. Weir structures were employed by Wilding et al. (1998) and Chen et al. (2008) to separate leukocytes from blood. Nagrath et al. (2007) succeeded to isolate circulating tumour cells from peripheral blood by using an affinity based separation technique. In such microfluidic devices the channels geometries become very complex, and sometimes the adhesion of the flowing cells to the channels walls causes problems. In order to control this phenomenon, one solution is to control chemical mediation between the flowing cells and the channel walls by use of surface coating. Cell adhesion could also be prevented by a proper exploitation of haemodynamic forces. In order to accomplish this, it is paramount to understand how the channel geometry affects adhesion. For this reason, we sought to investigate the adhesion phenomena in a microchannel with a complex geometry.

In this study, we used a confocal micro-PIV system to investigate the behaviour of RBCs and cancer cells in microchannels with geometrically symmetric bifurcation and confluences. We examined the asymmetry in the blood flow between the bifurcation and the confluence, which is unlike the Stokes flow of Newtonian fluid that should be symmetric in the microchannel. We observed asymmetry in the adhesion of cancer cells to channel walls even though the wall surface coating and the wall shear stress were almost symmetric between the bifurcation and the confluence.

2 Materials and methods

2.1 Confocal micro-PIV system

The confocal micro-PIV system used in this study and shown in Fig. 1 is the same as that described by Lima et al. (2006, 2009). Appendix A provides details of the system.

2.2 Microchannel

The microchannel was made of polydimethylsiloxane (PDMS) using a soft lithographic technique in the same manner reported by Fujiwara et al. (2009). The parent microchannel had a rectangular cross section 75 μm wide and 40 μm high whilst the daughter channel was 50 μm wide and 40 μm high. The bifurcation and confluence angles were 60° and the length of the straight channels after the bifurcation and before the confluence was 500 μm as shown in Fig. 2. The geometries of the bifurcation and the confluence were symmetric. The diameter of a RBC is about 8 μm, so the channel geometry is larger than the cell size.

The reservoir and the PDMS microchannel were coated with bovine serum albumin (BSA, 4 wt.%) using the same procedure described by Hou et al. (2009) to prevent any nonspecific adsorption of the cells to the channel wall

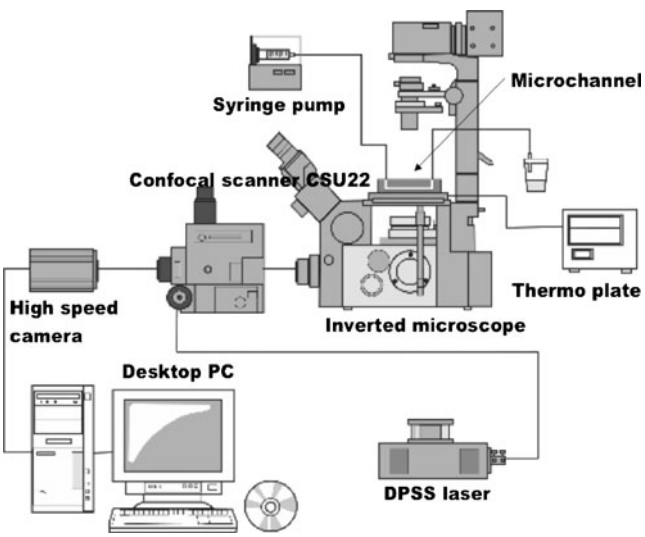

Fig. 1 Schematic of the experimental setup

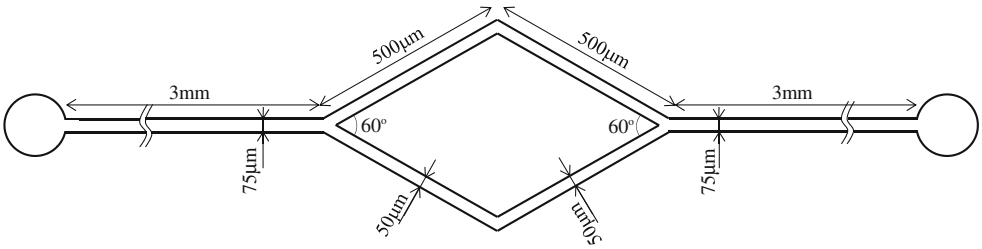

Fig. 2 Geometry of the PDMS microchannel

during the course of the experiment. In addition, as described in Section 3.3, the microchannel was coated with a sugar chain (1 mg/ml PVCA; Funakoshi Corp., Tokyo, Japan) in one test to examine its effect on the adhesion of cancer cells.

2.3 Fluids and cells

The RBCs were taken from a healthy 23-year-old male volunteer and centrifuged to separate the RBCs and plasma completely. They were then preserved at 4°C and dispersed in natural saline prior to the experiment. All procedures were carried out in compliance with the guidelines set by the Clinical Investigation Ethics Committee at Tohoku University.

The Cell Resource Centre for Biomedical Research at the Tohoku University Institute of Development, Aging and Cancer provided the B16 cancer cell line, which is popular as a mouse malignant melanoma cell line with high haematogenous metastasis potential. The cells were cultured in RPMI-1640 medium (Irvine Scientific, Santa Ana, CA, USA) containing 10% heat-inactivated foetal bovine serum (Gibco, Grand Island, NY, USA), 50 U/ml penicillin (Gibco) and 50 μg/ml streptomycin (Gibco) at 37°C in a humidified chamber under 5% CO_2. After culturing under an 80%–90% confluent condition, the cells were ready for the experiments described below. B16 cells have the diameter of about 15 μm.

Five kinds of working fluids were used in this study: pure water with 1% fluorescent particles 1 μm in diameter; dextran 40 (DEX40; low density dextran L 10% *w/w*; Otsuka Pharmaceutical Co. Ltd., Tokyo, Japan) with 10% hematocrit (Hct) human RBCs; DEX40 with 10% Hct human RBCs, in which 10% of the RBCs were labelled with fluorescent dye (C-7000; Molecular Probes, Carlsbad, CA, USA); phosphate-buffered saline (PBS(–); Gibco) with B16 cells (2.7×10^7 cells/μm); and PBS(–) with 10% human RBCs and B16 cells (2.7×10^7 cells/μm), in which the B16 cells were labelled with C-7000. The viscosity and the density of the DEX40 at 20°C were about 4.86×10^{-3} Pa·s and 1.05×10^3 kg/m^3, respectively. In the experiments described in Section 3.3, the DEX40, serum and plasma were also used as the solvent fluid for the B16 cells in one test to examine its effect on the adhesion of cancer cells.

The procedure for labeling both RBCs and cance cells was as follows: Centrifuge the blood sample (1 ml with 40% Hct) at 2,000 rpm for 5 min (Cancer cells: at 1,000 rpm for 5 min); Remove all PS and add 1 ml of fresh PS and 2 μl of cell tracker CM-Dil, C-7000 (50 μg, diluted with 50 μl of ethanol); Mix gently and incubate for 5 min at 37 °C, and then for 15 min at 4 °C; Wash cells with D-PBS; Centrifuge the solution (RBCs: 2,000 rpm, 5 min; Cancer cells: 1,000 rpm, 5 min) and remove the excess dye; Resuspend the washed cells in Dx-40 to the required RBC or cancer cells concentration by volume.

2.4 Experimental conditions

In the adhesion experiments using cancer cells, the centreline velocity of the straight part of the channel was 1.5 mm/s, and the Reynolds number was about 0.01. The average wall shear stress in the straight part was about 0.6 Pa, which was within the range of physiological conditions (Popel and Johnson 2005). In performing the confocal micro-PIV measurements, we maintained the centreline velocity at about 0.5 mm/s; we could not increase the velocity above that value due to a limitation of the PIV system. The microchannel was surrounded by adiabatic walls, and the temperature of the channel was maintained at 37°C using a thermo plate. The frame rate for the high-speed camera was 300 frames/s. Throughout this study, we observed the motion of the labelled RBCs and labelled B16 cells in the centre plane, i.e., 20 μm from the bottom. The tracer particles or fluorescently labeled cells were manually tracked through successive images by using a MtrackJ software (Meijering et al. 2006) as explained in Lima et al. (2009).

3 Results

3.1 Flow of pure water

We first investigated the flow field of pure water. We measured the trajectories of tracer particles by continuously tracking individual particles as shown in Fig. 3. We observed that the trajectories were almost symmetric for the bifurcation and confluence. This result is consistent

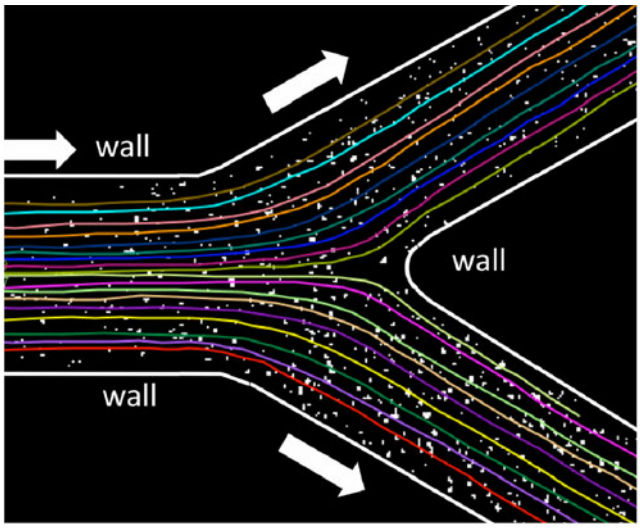

(a) at bifurcation

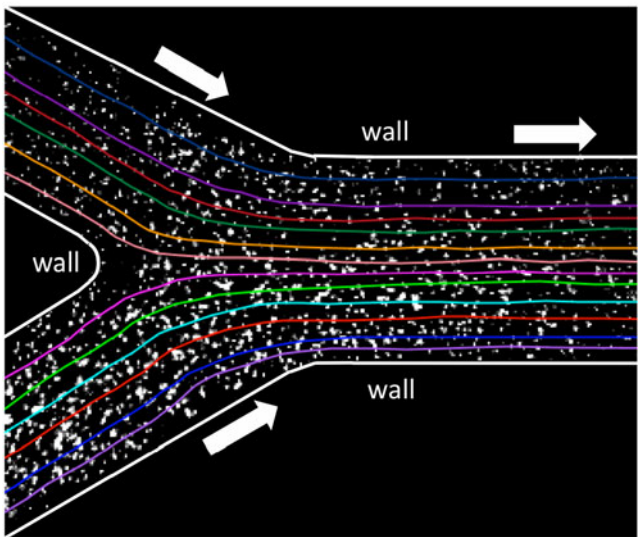

(b) at confluence

Fig. 3 Trajectories of 1-μm tracer particles in pure water measured at the centre plane of the microchannel. *Large arrows* in the figure indicate the flow direction. (**a**) at bifurcation (**b**) at confluence

with the Stokes flow condition, whereby the streamlines are symmetric if the geometry is symmetric as shown in Fig. 2.

3.2 Flow of 10% Hct blood

This section describes our investigation of blood flow. We first used a standard halogen light instead of the confocal system to observe distribution of RBCs and cell-free layers, as shown in Fig. 4. (Please see supplementary movies on the journal web site as well.) At the bifurcation (Fig. 4(a)), RBCs tended to collide with the inner wall where no cell-free layer was observed. RBCs near the outer wall, however, tended to flow away from the wall after the bifurcation where a cell-free layer was clearly present. The flow characteristics were completely different at the confluence. Figure 4(b) shows a triangular cell-free region just downstream of the apex of the inner wall, and cell-free layers were well developed on all walls around the confluence. These results indicate a strong asymmetry in the RBC distribution and in the cell-free layers between the bifurcation and the confluence, although the trajectories of tracer particles in pure water were almost symmetric.

The trajectories of labelled RBCs in the blood flow with 10% Hct were tracked in the centre plane and Fig. 5(a) shows the results at the bifurcation. RBCs initially located

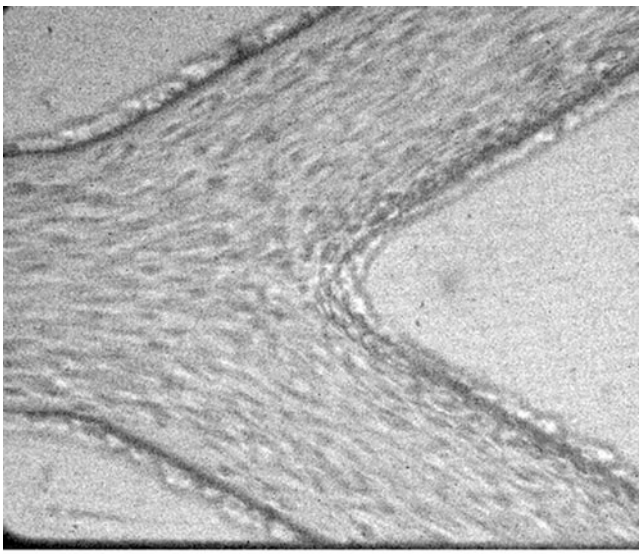

(a) at bifurcation

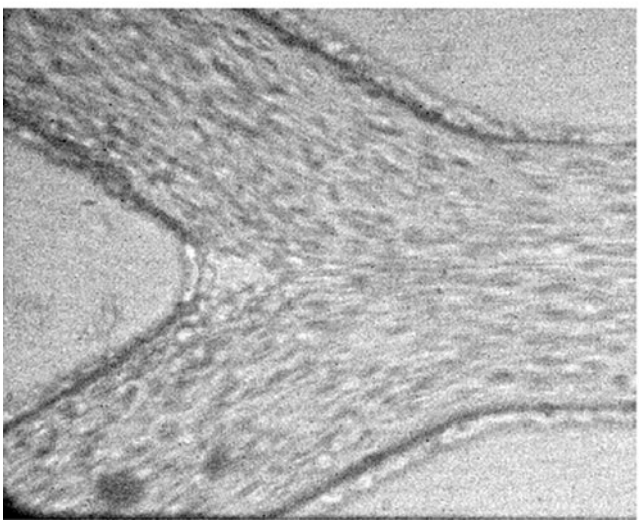

(b) at confluence

Fig. 4 Difference in the RBC distribution at the bifurcation and at the confluence. Supplementary movies can be found on the journal web site. (**a**) at bifurcation (**b**) at confluence

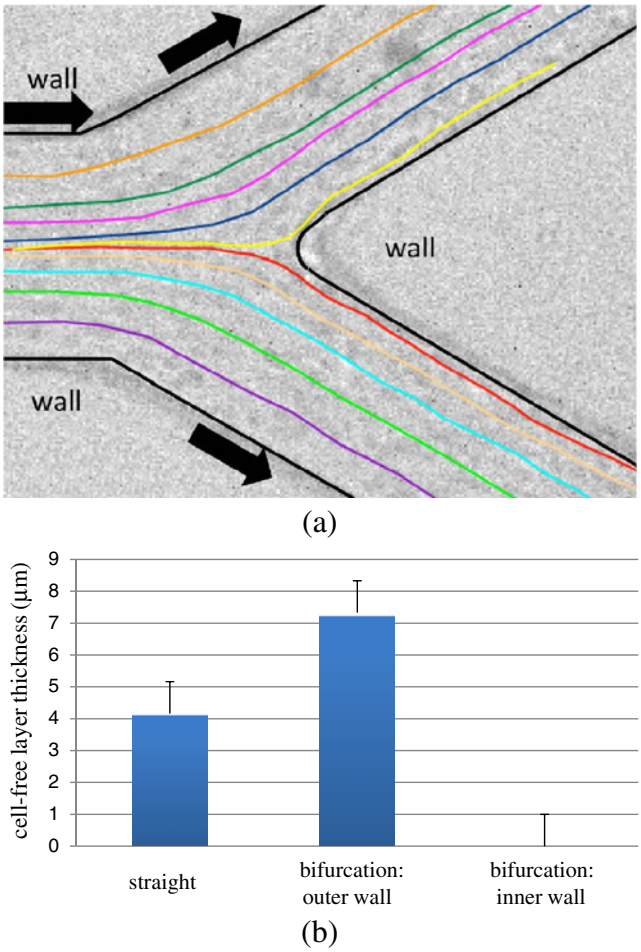

Fig. 5 RBC trajectories and cell-free layer around the bifurcation (Hct= 10%). (**a**) trajectories of labelled RBCs measured in the centre plane (**b**) distribution of cell-free layer thickness around the bifurcation. *Straight* indicates the position 50 μm upstream of the bifurcation whilst *bifurcation* indicates the position 50 μm downstream

near the centre of the straight channel could arrive very close to the inner wall of the bifurcation. RBCs initially near the wall, however, tended to flow away from the outer wall of the bifurcation. This behaviour is unlike that of tracer particles in pure water shown in Fig. 3(a).

To evaluate the flow field quantitatively, we measured the cell-free layer thickness around the bifurcation. Since the motions of RBCs were chaotic, the thickness of cell-free layer fluctuated considerably with time. Thus, we needed to employ statistical analysis to define the cell-free layer. The definition of the cell-free layer used in this study was the same as Fujiwara et al. (2009). We measured the distance between the wall and the RBC nearest the wall at 50 μm upstream or downstream of the bifurcation. We calculated the thickness of the cell-free layer by taking the average distance over about 50 RBCs per wall; Fig. 5(b) shows the results. The cell-free layer thickness increased on the outer wall after the bifurcation, but was zero on the inner wall.

3.3 Adhesion of cancer cells

We placed B16 cells in PBS(–) (without RBCs) and observed their motion in the microchannel coated by a sugar chain. Figure 6 shows the probability density of the spanwise (width) position of cancer cells 50 μm upstream from the bifurcation. Even though the cancer cells migrated slightly to the centre of the channel, they were distributed throughout the whole spanwise region. Cancer cells frequently adhered to the inner wall at the bifurcation as shown in Fig. 7. This figure shows a cancer cell flowing upstream (Fig. 7(a)) adhering to other cancer cells (Fig. 7 (b)), moving slightly on other cells, and then settling down (Fig. 7(c)). We performed similar experiments using DEX40, serum and plasma as the solvent fluid of the B16 cells as well as using BSA for coating. The effects of these conditions were not significantly different.

For a quantitative investigation of the probability of cancer cells adhering in the microchannel, we divided the microchannel into eight regions as shown in Fig. 8(a) and counted the number of adhering cancer cells in each region every minute. Figure 8(b) shows the results. We observed that the cancer cells tended to adhere to the inner wall at the bifurcation, i.e., in region D. The probability density distribution shows the strong asymmetry between the bifurcation and the confluence. In region D, cancer cells travelled very close to the wall in the same manner as the RBCs shown in Fig. 5(a), and this may be the reason why they adhered frequently in region D.

Last, we placed labelled B16 cells in PBS(–) with 10% human RBCs and observed the adhesion of cancer cells using the confocal micro-PIV system. We were successful

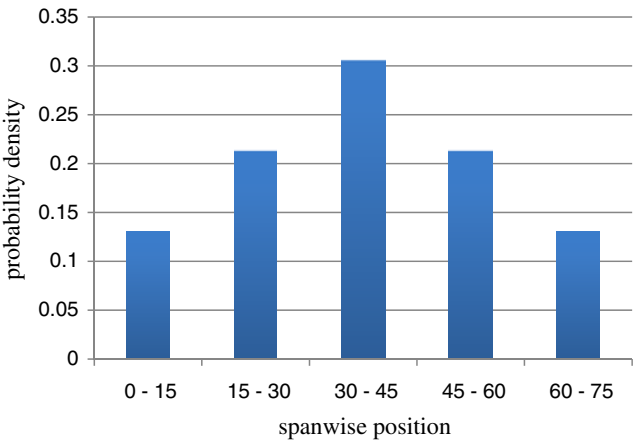

Fig. 6 Probability density of the spanwise position of cancer cells 50 μm upstream of the bifurcation. The experiments were performed using PBS(–) with cancer cells

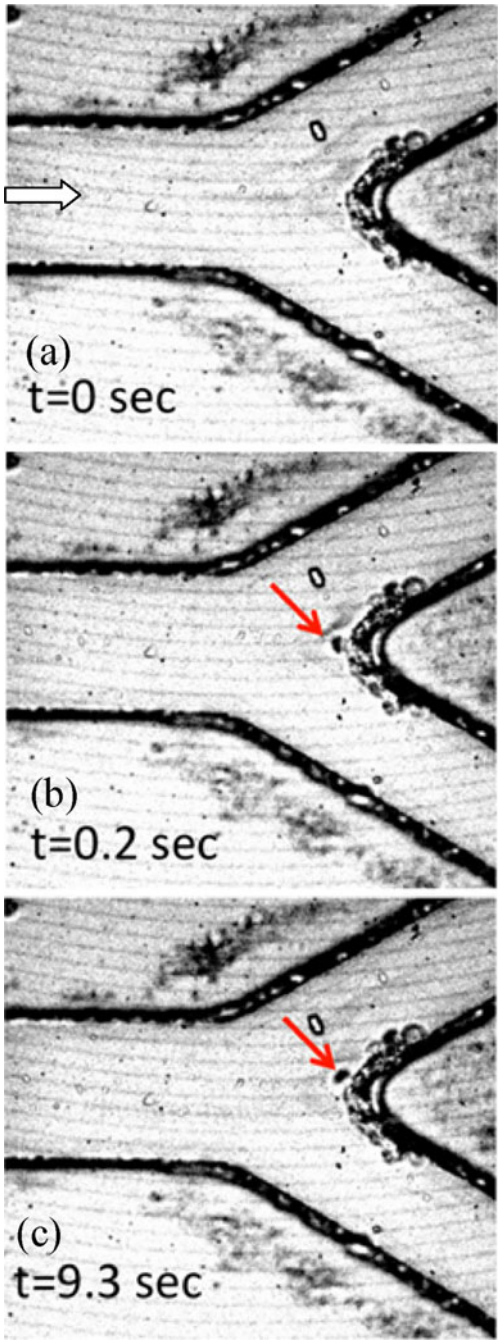

Fig. 7 Sequence of images showing cancer cell adhesion at the bifurcation: (**a**) a cancer cell comes from the inlet at the white arrow position, (**b**) the cell, indicated by the red arrow, adheres to other cancer cells at the bifurcation and (**c**) then settles down at the bifurcation. The experiments were performed using PBS(–) with cancer cells

in measuring the individual trajectories of cancer cells in blood flow using this system. Figure 9 shows a sample image of adhering cancer cells. Even when mixed with RBCs, the cancer cells adhered significantly to the inner wall of the bifurcation but very rarely around the confluence. Thus, the selective adhesion of cancer cells was not affected by the presence of RBCs.

4 Discussion

We detected strong asymmetry in the RBC motions and the cell-free layer between the bifurcation and the confluence, although the trajectories of tracer particles in pure water were almost symmetric. We observed similar asymmetry in blood flow in our previous study using a stenosed microchannel (Fujiwara et al. 2009). In that case, the trajectories of RBCs became asymmetric before and after the stenosis, and the cell-free layer thickness increased after the stenosis. In this study, however, the cell-free layer on the inner wall of the bifurcation disappeared, a different behaviour from that in the stenosed microchannel. These results indicated that the motions of RBCs were strongly influenced by the channel geometry.

In order to check the effect of the cross sectional area, we also performed similar experiments with a different channel geometry. In this case, the cross-sectional area before a bifurcation was 150×50 μm and after the bifurcation was 75×50 μm. Thus, the total cross sectional area was unchanged before and after the bifurcation. The results obtained in the study were actually not much different from the present study. This is because the cell-free layer and the adhesion of cancer cells are local phenomena near a wall, and the bulk flow has small effect on it if the wall shear stress is not too strong.

Asymmetry in particle trajectory does not occur if a single non-Brownian rigid sphere flows in a microchannel with symmetric geometry under the Stokes flow regime. The asymmetric trajectories found in this study were generated by the deformation of RBCs, the lift force of RBCs from the wall boundaries, the interactions between RBCs and the interactions between the cell surface and the wall surface. The deformation of RBCs and the lift force depended on the history of traction forces on the membrane along the trajectories. This was the cause of the asymmetry in RBC trajectories between the bifurcation and the confluence. Such asymmetry in blood flow is difficult to analyse computationally using conventional continuum approaches such as the Casson model (Casson 1959) because the blood cannot be considered a homogeneous fluid. Numerical methods are thus required to solve the motion of individual RBCs to investigate blood flow in complex microchannels. Another possibility to generate the asymmetric behaviours of cells is the opposite sign in the pressure gradient and the wall shear stress between the bifurcation and the confluence. Since the cells may respond to the gradient of the pressure and the stress, not only the magnitude of them but also the gradient of them may play a role. This should be investigated further in future studies.

The Peclet number for the mass transport of large molecules and platelets is often greater than unity (Ahuja

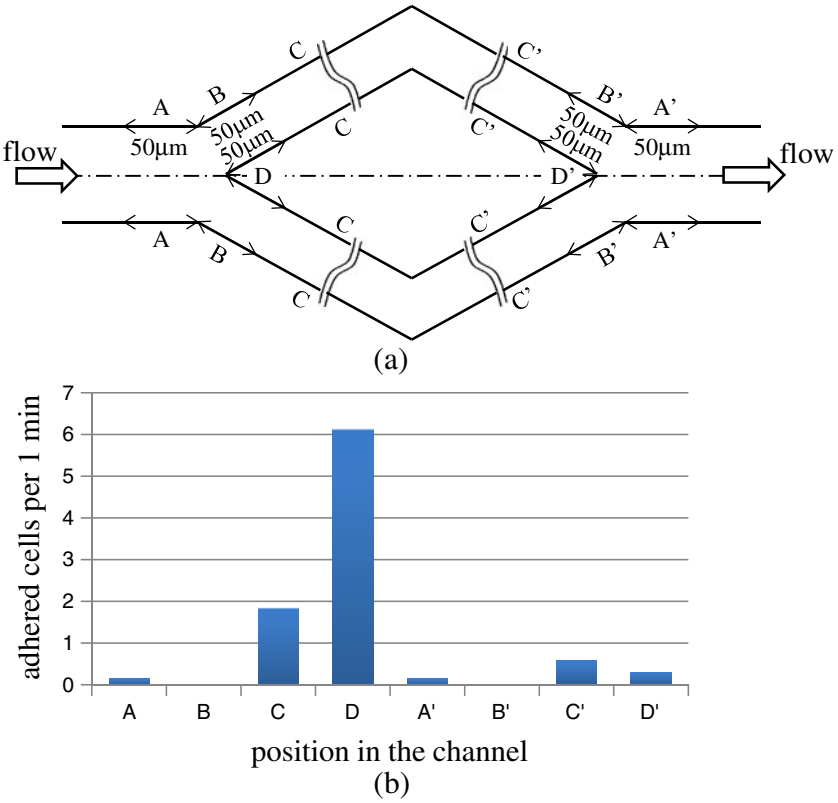

Fig. 8 Effect of wall position on the adhesion of cancer cells. The experiments were performed using PBS(–) with B16 cells (2.7×10^7 cells/μm). (**a**) channel wall divided into eight regions. *Large arrows* indicate the flow direction. (**b**) number of adhered cancer cells in the eight regions of the wall per minute

et al. 1978). The mass transport is thus not only governed by Brownian diffusion, but also by the microscale flow field generated by RBCs. The results of this study revealed that the cell-free layer increased on the outer wall after the bifurcation, but decreased on the inner wall. Thus, mass transport should be enhanced near the inner wall after the bifurcation, but reduced near the outer wall. This means that the effective diffusion coefficient for large molecules and platelets may vary spatially around the bifurcation. Previous studies have never explained such local changes in mass transport conditions around the bifurcation and the confluence in microcirculation and in biomedical microdevices.

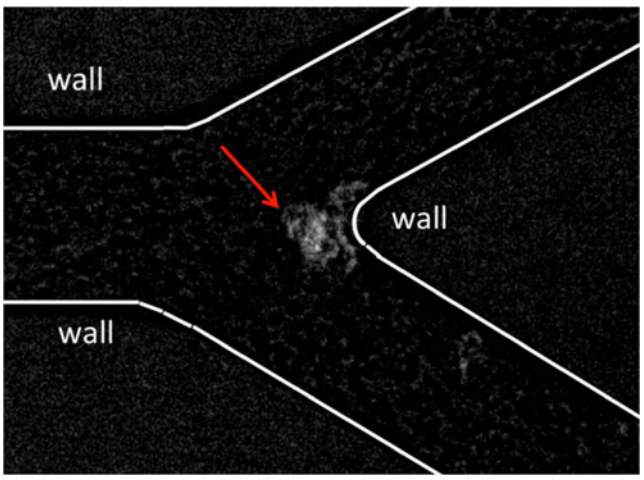

Fig. 9 Labelled cancer cells in blood adhering at the bifurcation. The *arrow* indicates the labelled cancer cells. The experiments were performed using PBS(–) with 10% human RBCs and B16 cells (2.7×10^7 cells/μm)

Microscale haemodynamics play an important role not only in transport phenomena but also in adhesion phenomena. In this study, we observed that B16 cells adhered mainly to the inner wall of the bifurcation but rarely near the confluence. Some previous studies have discussed the influence of wall shear stress on cancer cell adhesion, and the tendencies were distinctly different in cell lines with differing metastatic properties (Haier and Nicolson 2001). For example, A-549 lung carcinoma cells (Bastida et al. 1989) and MCF-7 human breast cancer cells (Moss et al. 1999) were found to experience enhanced adhesion to the endothelium due to the added mechanical stimulus of shear stress. In the microchannel used in this study, the wall shear stress was higher on the inner wall than on the outer wall at the bifurcation and the confluence. However, there should be no significant difference in the shear stress between the bifurcation and the confluence due to the symmetric channel geometry. Thus, the selective adhesion of B16 cells on the inner wall of the bifurcation was not due to the effect of shear stress. We believe that the cell-free layer thickness is a very important factor in the adhesion phenomena, and we will consider such detailed haemodynamics in future discussions.

Most previous cancer cell adhesion studies concentrated on chemical mediation. However, the results of this study indicated that microscale haemodynamics also play an important role in the adhesion of cancer cells. The effects of the solvent fluid of cancer cells (PBS(–), DEX40, serum or plasma) and the surface coating of the microchannel (no coating, BSA coating or sugar chain coating) were also investigated, but we observed no significant qualitative differences amongst them. Because the wall surface coating was symmetric between the bifurcation and the confluence, chemical mediation cannot explain the asymmetry in the cancer cell adhesion.

To confirm these conclusions, we also performed adhesion experiments in a stenosed microchannel like that used in our previous study (Fujiwara et al. 2009), instead of the microchannel with the bifurcation and the confluence. Cell-free layers developed in all regions of the stenosed microchannel, whilst low wall shear stress regions appeared upstream and downstream of the stenosis and high shear regions were observed around the stenosis (Fujiwara et al. 2009). The results of stenosed microchannel experiments showed that little adhesion of cancer cells occurred due to the existence of cell-free layers. Therefore, the cell-free layer as well as chemical mediation and wall shear stress all have important roles in the adhesion of cancer cells. These results provide the fundamental basis for a better understanding of blood flow and cell adhesion in biomedical microdevices.

Acknowledgments The authors are grateful for helpful discussions with Dr. R. Lima in Braganca Polytechnic Institute, and Prof. C. T. Lim in National University of Singapore. This study was supported by Grant-in-Aid for Scientific Research (S) from the Japan Society for the Promotion of Science (JSPS; No. 19100008) and by a Grant-in-Aid for Young Scientists (A) from the JSPS (No. 19686016). We also acknowledge the support from the 2007 Global COE Program "Global Nano-Biomedical Engineering Education and Research Network Centre".

Appendix A: Confocal micro-PIV system

The confocal micro-PIV system used in this study shown in Fig. 1 consisted of an inverted microscope (IX71; Olympus, Tokyo, Japan), a confocal scanning system (CSU22; Yokogawa, Tokyo, Japan), a high-speed camera (Phantom v7.1; Vision Research, Wayne, NJ, USA), a diode-pumped solid-state (DPSS) laser (Laser Quantum, Cheshire, UK), a syringe pump (KD Scientific, Holliston, MA, USA) to achieve constant flow, a thermo plate (Tokai Hit, Shizuoka, Japan) to control the temperature and an objective lens (magnification, 20×; N.A., 0.75; W.D., 0.17 mm; Olympus). The estimated thickness of the measurement plane (optical slice thickness) was 4.97 μm. By exposing the labelled cells to the laser, the system enabled us to track individual cells inside a blood flow of up to 20% Hct with high resolution and low optical thickness. The recorded images were evaluated in Image J (NIH, Bethesda, MD, USA) using the manual tracking MtrackJ plug-in.

References

A.S. Ahuja, W.R. Hendee, P.L. Carson, Transport phenomena in laminar flow of blood. Phys. Med. Biol. **23**, 928–936 (1978)

E. Bastida, L. Almirall, M.C. Bertomeu, A. Ordinas, Influence of shear stress on tumor-cell adhesion to endothelial-cell extracellular matrix and its modulation by fibronectin. Int. J. Cancer **43**, 1174–1178 (1989)

J.G. Beeson, S.J. Rogerson, B.M. Cooke et al., Adhesion of Plasmodium falciparum-infected erythrocytes to hyaluronic acid in placental malaria. Nat. Med. **6**, 86–90 (2000)

N. Casson, *Rheology of Disperse System* (Pergamon, London, 1959)

A.F. Chambers, A.C. Groom, I.C. MacDonald, Dissemination and growth of cancer cells in metastatic sites. Nat. Rev. Cancer **2**, 563–572 (2002)

X. Chen, D.F. Cui, C.C. Liu, H. Li, Microfluidic chip for blood cell separation and collection based on crossflow filtration. Sen. Actuators B **130**, 216–221 (2008)

J.A. DiVietro, D.C. Brown, L.A. Sklar, R.S. Larson, M.B. Lawrence, Immobilized stromal cell-derived factor-1alpha triggers rapid VLA-4 affinity increases to stabilize lymphocyte tethers on VCAM-1 and subsequently initiate firm adhesion. J. Immunol. **178**, 3903–3911 (2007)

R. Fahraeus, T. Lindqvist, The viscosity of the blood in narrow capillary tubes. Am. J. Physiol. **96**, 562–568 (1931)

I.J. Fidler, The pathogenesis of cancer metastasis: the 'seed and soil' hypothesis revisited. Nat. Rev. Cancer **3**, 453–458 (2003)

H. Fujiwara, T. Ishikawa, R. Lima, N. Matsuki, Y. Imai, H. Kaji, M. Nishizawa, T. Yamaguchi, Red blood cell motions in high-hematocrit blood flowing through a stenosed microchannel. J. Biomech. **42**, 838–843 (2009)

O.V. Glinskii, V.H. Huxley, G.V. Glinsky et al., Mechanical entrapment is insufficient and intercellular adhesion is essential for metastatic cell arrest in distant organs. Neoplasia **7**, 522–527 (2005)

J. Haier, G.L. Nicolson, Tumor cell adhesion under hydrodynamic conditions of fluid flow. Acta Pathol. Microbiol. Immunol. Scand. **109**, 241–262 (2001)

H.W. Hou, Q.S. Li, G.Y.H. Lee, A.P. Kumar, C.N. Ong, C.T. Lim, Deformability study of breast cancer cells using microfluidics. Biomed. Microdevices **11**, 557–564 (2009)

J. Kitayama, N. Tsuno, E. Sunami, T. Osada, T. Muto, H. Nagawa, E-selectin can mediate the arrest type of adhesion of colon cancer cells under physiological shear flow. Eur. J. Cancer **36**, 121–127 (2000)

S. Liang, M.J. Slattery, C. Dong, Shear stress and shear rate differentially affect the multi-step process of leukocyte-facilitated melanoma adhesion. Exp. Cell Res. **310**, 282–292 (2005)

S. Liang, M.J. Slattery, D. Wagner, S.I. Simon, C. Dong, Hydrodynamic shear rate regulates melanoma-leukocyte aggregation, melanoma adhesion to the endothelium, and subsequent extravasation. Ann. Biomed. Eng. **36**, 661–671 (2008)

R. Lima, S. Wada, K. Tsubota, T. Yamaguchi, Confocal micro-PIV measurements of three-dimensional profiles of cell suspension flow in a square microchannel. Meas. Sci. Technol. **17**, 797–808 (2006)

R. Lima, T. Ishikawa, Y. Imai, M. Takeda, S. Wada, T. Yamaguchi, Radial dispersion of red blood cells in blood flowing through glass capillaries: role of heamatocrit and geometry. J. Biomech. **41**, 2188–2196 (2008)

R. Lima, T. Ishikawa, Y. Imai, M. Takeda, S. Wada, T. Yamaguchi, Measurement of individual red blood cell motions under high hematocrit conditions using a confocal micro-PTV system. Ann. Biomed. Eng. **37**, 1546–1559 (2009)

E. Meijering, I. Smal, G. Danuser, Tracking in molecular bioimaging. IEEE Signal Process Mag. **23**, 46–53 (2006)

F.L. Miles, F.L. Pruitt, K.L. van Golen, C.R. Cooper, Stepping out of the flow: capillary extravasation in cancer metastasis. Clin. Exp. Metastasis **25**, 305–324 (2008)

S. Mine, T. Fujisaki, C. Kawahara et al., Hepatocyte growth factor enhances adhesion of breast cancer cells to endothelial cells *in vitro* through up-regulation of CD44. Exp. Cell Res. **288**, 189–197 (2003)

H. Mohamed, M. Murray, J.N. Turner, M. Caggana, Isolation of tumor cells using size and deformation. J. Chromatogr. A **1216**, 8289–8295 (2009)

M.S. Moss, B. Sisken, S. Zimmer, K.W. Anderson, Adhesion of non-metastatic and highly metastatic breast cancer cells to endothelial cells exposed to shear stress. J. Biorheology **36**, 359–371 (1999)

S. Nagrath et al., Isolation of rare circulating tumour cells in cancer patients by microchip technology. Nature **450**, 1235–1239 (2007)

G. Ostermann, K.S. Weber, A. Zernecke, A. Schroder, C. Weber, JAM-1 is a ligand of the beta(2) integrin LFA-1 involved in transendothelial migration of leukocytes. Nat. Immunol. **3**, 151–158 (2002)

A.S. Popel, P.C. Johnson, Microcirculation and hemorheology. Annu. Rev. Fluid Mech. **37**, 43–69 (2005)

C. Scholander, C.J. Treutiger, K. Hultenby, M. Wahlgren, Novel fibrillar structure confers adhesive property to malaria?infected erythrocytes. Nat. Med. **2**, 204–208 (1996)

S.J. Tan, L. Yobas, G.Y.H. Lee, C.N. Ong, C.T. Lim, Microdevice for the isolation and enumeration of cancer cells from blood. Biomed. Microdevices **11**, 883–892 (2009)

V. Thamilselvan, A. Patel, J.V. Zyp, M.D. Basson, Colon cancer cell adhesion in response to Src Kinase activation and actin-cytoskeleton by non-laminar shear stress. J. Cell. Biochem. **92**, 361–371 (2004)

P. Wilding, L.J. Kricka, J. Cheng, G. Hvichia, M.A. Shoffner, P. Fortina, Integrated cell isolation and polymerase chain reaction analysis using silicon microfilter chambers. Anal. Biochem. **257**, 95–100 (1998)